

## Concrete Reinforced with Graphene and Graphene Oxide

Yurov V.M.<sup>1</sup>, Zhangozin K.N.<sup>1</sup>, Portnov V.S.<sup>2</sup>, Rakhimova G.M.<sup>2\*</sup>, Rakhimov A.M.<sup>2</sup>.

<sup>1</sup>"Vostok" LLP, Astana, Kazakhstan

<sup>2</sup>Abylkas Saginov Karaganda Technical University, Karaganda, Kazakhstan

\*corresponding author

**Abstract.** In this paper, we propose a model of concrete reinforced with graphene and graphene oxide. The thickness of the surface layer of the C–S–H gel is  $R(I) = 60.3 \text{ nm}$  ( $< 100 \text{ nm}$ ), i.e. it is a nanostructure according to Gleiter. The equation we obtained shows that the higher the adhesion energy  $W_a$ , the more difficult it is to destroy a solid. This means that concrete is easier to destroy by bending than by compression ( $W_{aa} > W_{ac}$ ). The  $R(II)$  layer, which we called the mesolayer, is stronger than the  $R(I)$  layer, since  $\gamma_2 = 3\gamma_1$ . It differs from the nanolayer and the bulk phase in that the size effects in it occur according to a different type. Here, size effects of the kinetic type are present, associated with temperature, the mean free path of elementary excitations, etc., but they do not exceed 1 micron. At  $h = R(I)$ , a second-order phase transition (according to Ehrenfest) occurs, the nature of which is described by us using the Landau mean field method. There are no size effects in the bulk phase (larger than 1 micron). It is shown that graphene and graphene oxide are introduced into the interlayer space. Graphene and GO, limited in the interlayer region of the C–S–H gel, demonstrate different morphology. In graphene, carbon atoms, ordered in the  $xy$  plane, are distributed far from the C–S–H surface. No expansion along the  $z$ -direction is observed. The C–C bonds in GO are stretched in the  $z$ -direction, and the graphene sheet is somewhat damaged. Compared to standard concrete, the  $R(I)$  and  $R(II)$  values decrease by half and the elastic parameters of concrete change. The article shows that the addition of graphene and graphene oxide to cement mortar significantly strengthens (by 4-5 times) standard concrete.

**Keywords:** concrete, graphene, nanolayer, mesolayer, size effect, strength

### Introduction

Reference [1] (see bibliography therein) presents graphene (G) reinforced concrete. It shows an extraordinary increase in compressive strength of up to 146%, flexural strength of up to 79.5% and a 78% reduction in maximum displacement due to compressive load. At the same time, improved electrical and thermal performance is found with an 88% increase in heat capacity. A significant reduction in water permeability of almost 400% compared to standard concrete, which is an extremely desirable property for the long-term durability of concrete structures, makes this new composite material ideal for construction in flood-prone areas. Finally, it is shown that the incorporation of G into modern concrete will result in a 50% reduction in the required concrete material, while still meeting building load specifications. This will result in a significant reduction in carbon emissions from cement production of 446 kg/tonne.

In the work [2] (see bibliography therein) graphene oxide (GO) reinforced concrete was presented. The current study showed that the inclusion of GO even with 0.02% by weight of cement increased the strength by 12-24% and durability properties. The inclusion of GO can accelerate the hydration process of cement as it provides nucleation sites for cement hydrates. But the workability was reduced by 4% due to the agglomeration of GO, causing the water molecule to remain trapped. The water permeability properties tend to decrease with increasing GO content. And the quality of concrete mixtures was improved as the microstructural analysis of the mixtures actually indicates that GO acts as a filler of the material, healing the microcracks at the nanoscale, helping to transport water to the unreacted cement particles.

A review of all previous studies on G and GO reinforced concrete was made in [3]. It was shown that there are four forms of graphene products, namely graphene (G), graphene oxide (GO), reduced graphene oxide (rGO) and graphene nanoplatelets (GNPs), as shown in Fig. 1. These forms of graphene products have been used in numerous studies including [1, 2]. Emphasis is placed on the problems associated with G, GO, rGO and GNP reinforced concrete. These problems are as follows: G, GO reduce the workability of concrete and the mechanisms for its reduction are unclear; there remains a problem of the quality of carbon nanostructures leading to the development of microcracks; the production of graphene with controlled quality at low cost on an industrial scale is a big challenge; the inability of graphene to achieve high dispersion can potentially have an adverse effect on the properties of concrete due to the formation of agglomerates and weak pockets; graphene oxide can be a hazardous material since it can cause an explosion under certain conditions.

## 1. Methods and Materials

### 1.1 Experimental methodology

This study utilized a combination of experimental and theoretical approaches to examine the structure and

properties of concrete reinforced with graphene and graphene oxide. The research aimed to assess how these nanomaterials influence the mechanical and microstructural characteristics of concrete. The methodology was divided into two main components: experimental investigations and theoretical modeling.

The experimental portion of the study involved the preparation of concrete samples with varying concentrations of graphene and graphene oxide. The mixing process followed standardized procedures to ensure homogeneous dispersion of the nanomaterials. To evaluate their impact, multiple tests were conducted:

Compression and flexural strength tests were performed using a hydraulic press to assess load-bearing capacity and durability. Atomic force microscopy (AFM) and scanning electron microscopy (SEM) were employed to observe the dispersion of graphene within the concrete matrix and its interaction with calcium silicate hydrate (C–S–H) gel. X-ray diffraction (XRD) and energy-dispersive spectroscopy (EDS) were utilized to study phase composition and elemental distribution, ensuring proper integration of graphene-based additives. A slump test was conducted to examine the effects of graphene on the fluidity and workability of fresh concrete mixtures.

Concrete sample preparation followed GOST 10180-2012 standards to ensure reliable and reproducible results.

## 1.2 Materials

The primary materials used in this study included:

- cement: Portland cement CEM I 42.5N, chosen for its high compressive strength and optimal hydration characteristics;
- graphene and Graphene Oxide: These nanomaterials were introduced in concentrations ranging from 0.02% to 0.15% by cement mass, carefully dispersed to prevent agglomeration;
- aggregates: Natural sand (0.1–4 mm particle size), gravel, and crushed stone were used as fillers;
- water: Distilled water was utilized to eliminate the influence of impurities on hydration reactions;
- chemical Additives: In selected trials, plasticizers and superplasticizers were added to optimize the rheology and workability of the concrete mixture.

Theoretical analysis was conducted using molecular dynamics simulations to investigate the interaction of graphene and graphene oxide with C–S–H gel at the nanoscale.

The combined experimental and theoretical approaches provided valuable insights into the reinforcing effect of graphene and graphene oxide on concrete. The integration of these nanomaterials was shown to enhance mechanical strength, reduce crack formation, and improve durability. The findings contribute to the ongoing development of advanced, high-performance concrete materials with superior structural properties.

## 2. Results and discussion

The above issues include production consistency, cost of graphene-based additives, dispersion of graphene in concrete, workability and flowability of graphene-based concrete, sustainability, and safety issues.

We also reported in [4] on improving the properties of graphene-added concrete obtained by liquid-phase exfoliation of graphite [5].

**The aim** of this paper is to propose a model of graphene and graphene oxide reinforced concrete.

### Nano-meso-macrostructure of concrete

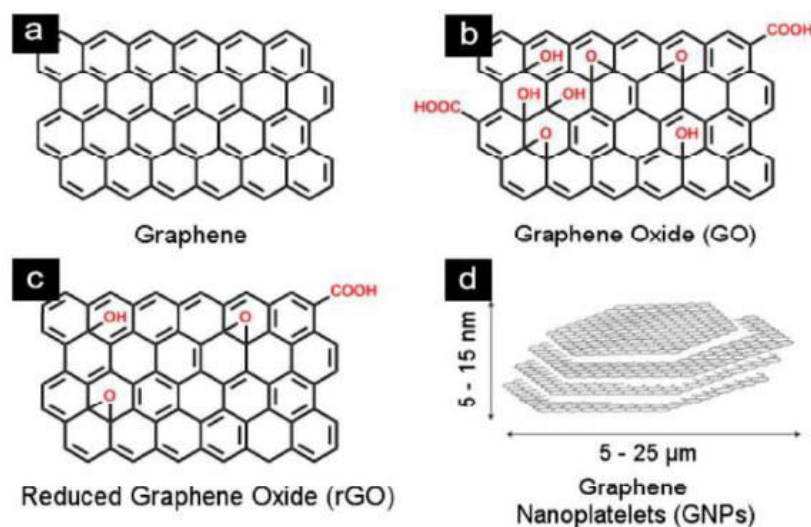
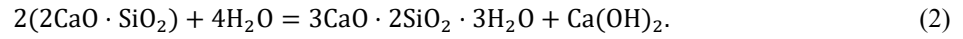


Fig. 1. - Illustration of (a) graphene (G), (b) graphene oxide (GO), (c) reduced graphene oxide (rGO), and (d) graphene nanoplatelets (GNPs) [3]

Concrete consists of cement paste, which is a porous and hierarchical material with different phases. When cement powder is mixed with water, a hydration reaction results in the formation of the main chemical products: calcium silicate hydrate (C–S–H), calcium hydroxide (CH), ettringite, and monosulfoaluminate. C–S–H accounts for approximately 70% of the fully hydrated products and is the main contributor to the mechanical strength of the material [6]. The silicate phases react with water to form calcium hydroxide and a rigid calcium silicate hydrate gel, the C–S–H gel [7]:



The thickness of the surface layer of a solid body R(I) is given by the formula [8]:

$$R(I) = 0,17 \cdot 10^{-9} \cdot \alpha \cdot v[m]. \quad (3)$$

In equation (3) it is necessary to know one parameter – the molar volume of the element, which is equal to  $v = M/\rho$  (M is the molar mass,  $\rho$  is its density),  $\alpha = 1 \text{ m}^{-2}$  is a constant to maintain the dimensionality (R(I) [m]). Considering that the rigid calcium silicate gel of the C–S–H hydrate is a homogeneous solid solution, it is easy to estimate the molar mass from equations (1) and (2) –  $M_1 = 1070 \text{ g/mol}$ ;  $M_2 = 922 \text{ g/mol}$ . The crystal structure obtained from equation (2) is closer to the mineral tobermorite [9], which is a layered crystalline form of calcium silicate. The density of the C–S–H gel is closely related to the water content in the pores of the gel. Neutron and X-ray scattering methods were used to determine with high accuracy [10] the density and water content in saturated globules. The density is  $2.604 \text{ g/cm}^3$ ,

The thickness of the surface layer of the C–S–H gel according to equation (3) is -  $R(I) = 60.3 \text{ nm}$ , and the number of layers is  $n = R(I)/a$  (a is the interlayer distance, equal to  $a = 1.4 \text{ nm}$  [7]). This means that the number of C–S–H layers is  $n = 43$ . According to our work [8], the diagram of the crystalline form of calcium silicate will look like that shown in Fig. 2a, and the silicate chain (monolayer of calcium silicate) is shown in Fig. 2b.

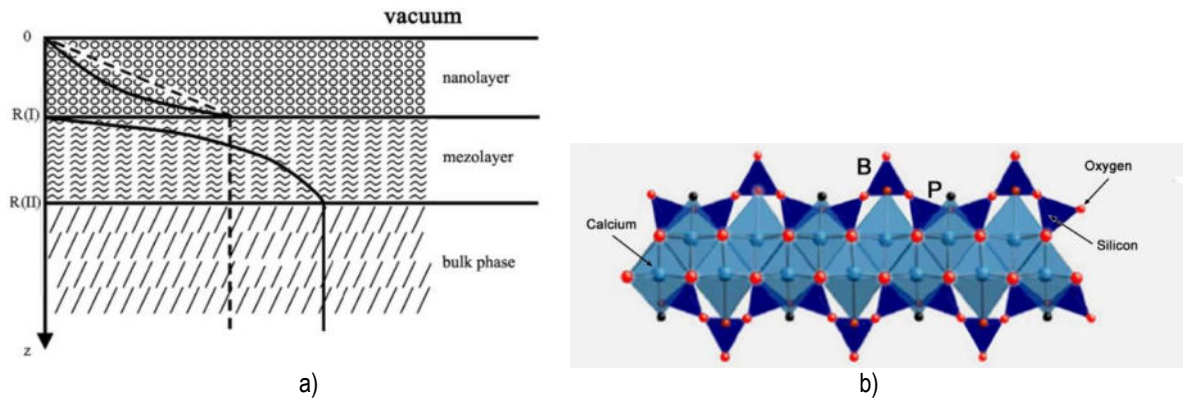


**Fig. 2.** - Schematic diagram of a solid: nanolayer → mezolayer → bulk phase (a); schematic diagram of a C–S–H layer showing a Ca–O core layer with a silicate tetrahedron attached on both sides. The silicate chain, calcium octahedron and oxygen atoms are shown as dark blue, light blue tetrahedron and red spheres, respectively (b) [7].

The thickness of the surface layer of the C–S–H gel is  $R(I) = 60.3 \text{ nm}$  ( $< 100 \text{ nm}$ ), i.e. it represents a nanostructure according to Gleiter [11]. The C–S–H gel in water forms crystalline nuclei with a critical radius [12]:

$$r_c = 2 M \gamma_{12} T_0 / \rho q \Delta T, \quad (4)$$

where M is the molar mass;  $\gamma_{12}$  is the surface tension at the boundary; T is the temperature;  $\rho$  is the density; q is the heat of fusion. Our estimate gives  $r_c = 5 \text{ nm}$ , which means that the R(I) layer contains  $n\Gamma = R(I)/r_c \approx 12$  globules. This situation is shown using atomic force microscopy (AFM) in Fig. 3.

Size effects in the R(I) layer are determined by a collective of atoms (collective processes). Such “semi-classical” size effects are observed only in nanostructures [13].

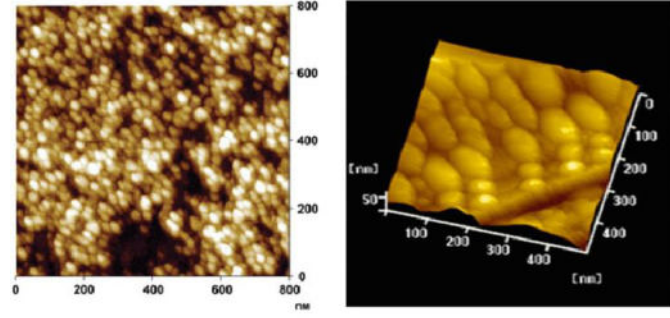


Fig. 3. - AFM photographs of C-S-H particles [7].

This means that the R(I) layer is a nanolayer (Fig. 2a). The surface energy of a bulk crystal  $\gamma_2$  is equal to [14]:

$$\gamma_2 = 0,7 \cdot 10^{-3} \cdot T_m [\text{J/m}^2], \quad (5)$$

where  $T_m$  is the melting temperature (K).

In the R(I) layer, the size effect must be taken into account and the surface energy becomes equal to  $\gamma_1$  [14]:

$$\gamma_1 = \gamma_2(1 - R(I)/R(I) + h) \approx 0,3\gamma_2. \quad (6)$$

Equation (6) shows that the surface energy of the R(I) layer is three times less than the surface energy of the main crystal. To separate the R(I) layer from the rest of the crystal, energy must be expended, which is called the adhesion energy [15]:

$$W_a = \gamma_1 + \gamma_2 - \gamma_{12} \approx \gamma_1 + \gamma_2 = 1,3\gamma_2, \quad (7)$$

where  $\gamma_{12}$  is the surface energy at the phase boundary, which is negligibly small due to the second-order phase transition.

The internal stresses  $\sigma_{is}$  between phases  $\gamma_1$  and  $\gamma_2$  can be calculated using the formula [16]:

$$\sigma_{is} = \sqrt{W_a \cdot E/R(I)}, \quad (8)$$

where  $E$  is the Young's modulus of elasticity. Using equations (5)–(8), we calculate the elastic parameters for standard concrete using a layered structure such as tobermorite or calcium silicate.

Table 1. Elastic parameters of standard concrete

Concrete	$W_{aa}$ , J/m <sup>2</sup>	$W_{ac}$ , J/m <sup>2</sup>	$\sigma_{isa}$ , MPa	$\sigma_{isc}$ , MPa	$E_a$ , GPa	$E_c$ , GPa
C-S-H ( $\rho = 2,604$ )	4,517	1,654	5589	1334	142	65

The melting point of calcium silicate is  $T_m = 1817$  K and  $\gamma_2 = 1272$  mJ/m<sup>2</sup>, Young's modulus  $E = 65$  GPa for C-S-H [7]. Significant elastic stresses in the R(I) layer lead to the creation of nanocracks, the length of which is  $L_{nm} = R(I)$  [14].

For the destruction of a solid, force, deformation and energy criteria of destruction were developed. There is the following relationship between them [17]:

$$\frac{K_{1c}^2(1-\mu^2)}{E} = 2\delta_{1c}\sigma_B = G_{1c} = J_{1c} = 2\gamma = W_a, \quad (9)$$

where  $K_{1c}$  is the critical stress intensity factor, the force criterion of destruction;  $E$  is the elastic modulus;  $\mu$  is Poisson's ratio;  $\delta_{1c}$  is the critical opening at the crack tip, the deformation criterion of destruction;  $\sigma_B$  is the ultimate strength;  $G_{1c}$  is the critical intensity of the released energy, the energy criterion of destruction;  $J_{1c}$  is the critical J-integral, the energy criterion of destruction;  $\gamma$  is the surface energy,  $W_a$  is the adhesion energy.

Equation (9) shows that the greater  $W_a$ , the more difficult it is to destroy a solid. This means that concrete is easier to destroy by bending than by compression ( $W_{aa} > W_{ac}$ ).

The R(II) layer, which we called the mesolayer (Fig. 2a), is stronger than the R(I) layer, since  $\gamma_2 = 3\gamma_1$ . It differs from the nanolayer and the bulk phase in that the size effects in it occur in a different way. Here, size effects of the kinetic type are present, related to temperature, the mean free path of elementary excitations, etc., but do not exceed

1 micron. At  $h = R(I)$ , a second-order phase transition occurs (according to Ehrenfest), the nature of which we described in [18] using the Landau mean field method. In the bulk phase (larger than 1 micron), there are no size effects.

**Concrete reinforced with graphene and graphene oxide.**

The structure of C–S–H obtained by molecular dynamics (MD) [7] with graphene (G) and graphene oxide (GO) is shown in Fig. 4a, b.

It can be seen from Fig. 4 that graphene and graphene oxide are embedded in the interlayer space. Graphene and GO confined in the interlayer region of C–S–H gel exhibit different morphologies.

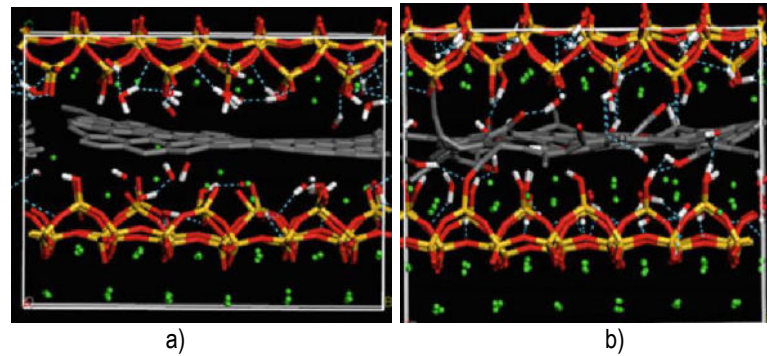


Fig. 4. - Structure of G/C–S–H and GO/ C–S–H [7].

In graphene, the carbon atoms, which are ordered in the xy plane, are distributed away from the C–S–H surface. No expansion along the z-direction is observed at the graphene/C–S–H interface in Fig. 4a. On the other hand, as shown in Fig. 4b, the protruding hydroxyls on both sides of GO indicate the C–S–H interface. The C–C bonds in GO are stretched in the z-direction, and the graphene sheet is somewhat disrupted. Compared with standard concrete, the  $R(I)$  and  $R(II)$  values are halved and the elastic parameters of concrete change. These changes are shown in Table 2. Concrete consists of components in the following weight proportions: water 10%, cement 20%, fillers (sand, gravel, crushed stone) 70%. The concentration of graphene during the formation of the concrete mixture drops by 3 times, i.e., in an aqueous solution, the concentration of graphene will be 0.15%. For  $1\text{m}^3$  of concrete (= 2 tons) we get 300 g of graphene.

Table 2. Elastic parameters of concrete with graphene and graphene oxide.

Concrete	$W_{aa}, \text{J/m}^2$	$W_{ac}, \text{J/m}^2$	$\sigma_{isa}, \text{MPa}$	$\sigma_{isc}, \text{MPa}$	$E_a, \text{GPa}$	$E_c, \text{GPa}$
graphene	17,243	6,314	25000	6250	1100	525
graphene oxide	14,629	5,418	10392	2598	430	197

Comparison of Tables 1 and 2, as well as equation (9), we conclude that the addition of graphene and graphene oxide to cement mortar significantly strengthens (by 4-5 times) standard concrete. In Table 2,  $T_m = 4510 \text{ K}$  is chosen for the melting temperature of graphene [19].

Due to the compositional, structural and physical complexity of the C–S–H gel, the main building blocks of cement hydrate have not yet been fully understood [7].

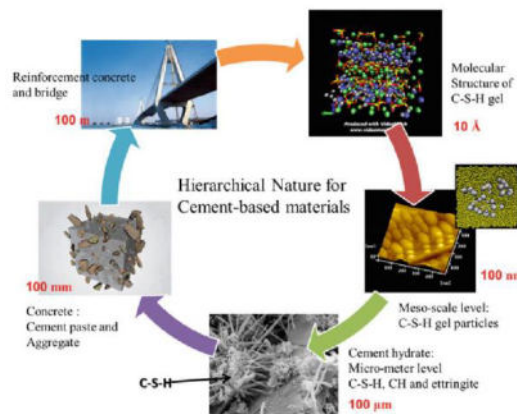


Fig. 5.- Hierarchical structure of concrete [7]

As shown in Fig. 5, at the macroscale ( $>10^{-3}$  m), concrete can be regarded as a material consisting mainly of two phases: aggregate and cement matrix. At the microscale ( $10^{-3} - 10^{-6}$  m), different hydration products and different C–S–H gel morphologies form a heterogeneous structure of cement paste. At the mesoscale, less than 1  $\mu\text{m}$ , the C–S–H gel can be observed as elliptical-shaped particles packed with different densities. At the nanoscale ( $<10^{-9}$  m), the distribution and arrangement of Ca, Si, OH form the basic C–S–H structure. Concrete, the most widely used building material, has been applied to pavements, architectural structures, foundations, highways, roads, overpasses, parking structures, brick, block walls, and foundations for gates, fences, and pillars. And its use is not comparable with other materials [20].

## Conclusion

One of the pressing issues in the mining industry of Kazakhstan is the processing of technogenic mineral formations (TMF). Currently, more than 60 billion tons of TMF have been accumulated in Kazakhstan [21]. At the same time, the total annual level of TMF processing is about 11% of the annual output, while in developed industrial countries the level of industrial waste use reaches 70–80% [22]. In our opinion, TMF processing should be carried out by creating modified concrete from TMF with an admixture of graphene or graphene oxide, the most widely used building material.

## Acknowledgments

This scientific article was published as part of the grant funding for 2024–2026 IRN No. AR32488258 "Development of an innovative technology for obtaining graphene by intercalating graphite with microcluster water and modifying HTSC ceramics with graphene" (the study is funded by the Science Committee of the Ministry of Science and Higher Education of the Republic of Kazakhstan).

## References

- [1] Dimov D., Amit I., Gorrie O., Barnes M.D., Townsend N.J., Neves A.I.S., Withers F., Russo S. and Craciun M.F. Ultrahigh Performance Nanoengineered Graphene-Concrete Composites for Multifunctional Applications // *J. Advanced Functional Materials*, 2018, V. 28, № 23. - P. 1705183. h DOI: <http://hdl.handle.net/10871/32568>
- [2] Devi S.Ch., Khan R.A. Mechanical and durability performance of concrete incorporating graphene oxide // *Journal of Materials and Engineering structures*, 2019, Vol. 6. – P. 201–214.
- [3] Fayyad T.M., Abdalqader A.F., Sonebi M. An insight into graphene as an additive for the use in concrete // *Civil Engineering Research in Irtland*, 2022. – P. 67-72.
- [4] Zhangozin K.N. *Methodus nova graphene producendi cum aqua microcluster intercalata.* – Almaty : Darkhan, 2023. – 102 p.
- [5] Zhangozin K.N., Zhanabergenov T.K., Kargin D.B. Circa novam methodum producendi pulveris graphene // *Nomenclator ENU dictus est. L. Gumileva*, 2021, tomi CXXXVI, N. III. - P. 8-16. DOI: <https://doi.org/10.32523/2616-6836-2021-136-3-8-16>
- [6] Richardson I.G. The calcium silicate hydrates // *Cement and Concrete Research*, 2008, Vol. 38(2). – P. 137–158. doi:10.1016/j.cemconres.2007.11.005
- [7] Hou D. *Molecular Simulation on Cement-Based Materials. From Theory to Application.* - Science Press and Springer Nature Singapore Pte Ltd. 2020. – 197 p. <https://doi.org/10.1007/978-981-13-8711-1>
- [8] Yurov V.M., Portnov V.S., Maussymbayeva, A.D. Thickness of the surface layer as-class hydrocarbons// *Aspectibus physico-chemicis investigandi racemis, nanostructuris et nanomaterialibus.* — 2022. — Soboles. 14. - pp. 331-341. DOI: 10.26456/pcascnn/2022.14.331.
- [9] Hamid S. The crystal structure of the 11 A natural tobermorite  $\text{Ca}_2.25\text{Si}_3\text{O}_7.5(\text{OH})1.5\cdot\text{H}_2\text{O}$  // *Zeitschrift für Kristallographie*, 1981, Vol. 154. - P. 189–198 DOI:10.1524/zkri.1981.154.14.189.
- [10] Allen A.J., Thomas J.J. and Jennings H.M. Composition and density of nanoscale calcium silicate hydrate in cement // *Nature Material*, 2007, Vol. 6. – P. 311–316. DOI:10.1038/nmat1871
- [11] Gleiter H. Nanostructured materials: basic concepts and microstructure // *Acta mater.*, 2000, V. 48. - P. 1-29. DOI:10.1016/S1359-6454(99)00285-2
- [12] Volmer M. *Kinetics formationis novi periodi.* - M.: Nauka, 1986. - 208 p.
- [13] Uvarov N.F., Boldyrev V.V. Magnitudo effectus in chymiae systemata heterogeneorum // *Uspekhi khimii*, 2001, T. 70 (4). - pp. 307-329. (In Russian). DOI: <https://doi.org/10.1070/RC2001v070n04ABEH000638>
- [14] Yurov V.M., Goncharenko V.I., Oleshko V.S. Studium primarium nanocracks in atomicis metallis levibus // *Physica Technical Epistolae.* - 2023. - Volumen 49. - Quaestio. 8. - pp. 35-38. DOI: 10.21883/PJTF.2023.08.55136.19504
- [15] Yurov V., Zhangozin K. Surface layer thickness, defects and strength of graphite // *The scientific heritage*, 2023, No 128. – P. 20-27. DOI:10.53939/1560-5655\_2024\_1\_19
- [16] Yurov V., Zhangozin K. About the mechanism of graphite splitting // *International independent scientific journal*, 2024, №58. – P. 29-40. DOI:10.53939/1560-5655\_2024\_1\_19

- [17] Erasov V.S., Oreshko E.I. Rationes dependentiae notarum mechanicarum rimae resistentiae materialis in magnitudine materiae Aviation specimen // Aviation materials and technologies, 2018, n. 3(52). - P. 56-64. DOI: 10.18577/2071-9140-2018-0-3-56-64
- [18] Yurov V.M., Guchenko S.A., Laurinas V.Ch., Zavatskaya O.N. Structural phase transition in a surface layer of metals // Bulletin of KarSU, 2019, – №1. – С. 50-60. DOI:10.31489/2019PH1/50-60
- [19] Los J.H., Zakharchenko K.V., Katsnelson M.I. and Fasolino A. Melting temperature of graphene // Phys. Rev., 2015, B91, 045415. DOI: <https://doi.org/10.1103/PhysRevB.91.045415>
- [20] Rakhimova G., Slavcheva G., Aisanova M., Rakhimov M., Tkach E. The influence of a complex additive on the strength characteristics of concrete for road construction // International Journal of GEOMATE. – 2023. 25 (110), pp.243-250. DOI: <https://doi.org/10.21660/2023.110.3934>
- [21] Mashkin N.A., Esirkepova A.B., Sherov K.T., Rakhimova G.M., Zharkevich O.M., Mussayev M.M. Activation of Cement Binder in Heavy Concrete Technology //Material and Mechanical Engineering Technology, 2020 (3), 9–12.
- [22] Fakhrullin R. F., Tursunbayeva A., Portnov V. S., L'vov Yu. M. Ceramic Nanotubes for Polymer Composites with Stable Anticorrosion Properties // Crystallography Reports, 2014 (7) Vol. 59, 1107–1113. DOI: <https://doi.org/10.1134/S1063774514070104>

### Information of the authors

**Yurov Viktor Mikhailovich**, Candidate of Physical and Mathematical Sciences, Associate Professor, leading construction manager of LLP “Vostok”  
e-mail: [exciton@list.ru](mailto:exciton@list.ru)

**Zhangozin Kanat Nakoshevich**, Director, Leading Researcher of TSK-Vostok LLP, Candidate of Physical and Mathematical Sciences, Associate Professor, e-mail: [4kzh@mail.ru](mailto:4kzh@mail.ru),

**Portnov Vassily Sergeevich**, Doctor of Technical Sciences, Professor, Abylkas Saginov Karaganda Technical University  
e-mail: [vs\\_portnov@mail.ru](mailto:vs_portnov@mail.ru)

**Rakhimova Galiya Mukhamedievna**, Candidate of Technical Sciences, Associate Professor of the Department of Construction Materials and Technologies of the Abylkas Saginov Karaganda Technical University  
e-mail: [g.rakhimova@kstu.kz](mailto:g.rakhimova@kstu.kz)

**Rakhimov Askhat Muratovich**, PhD, senior lecturer of the Department of Construction Materials and Technologies of the Abylkas Saginov Karaganda Technical University  
e-mail: [rakhimov.askhat@gmail.com](mailto:rakhimov.askhat@gmail.com)